

Fe–Pt Twisted Heterometallic Bicyclic Supramolecules via Multicomponent Self-Assembly

Hajar Sepehrpour,* Manik Lal Saha,* and Peter J. Stang*

Department of Chemistry, University of Utah, 315 South 1400 East, Room 2020, Salt Lake City, Utah 84112, United States

S Supporting Information

ABSTRACT: Herein, we describe a novel multicomponent self-assembly approach that has the prospect of furnishing unprecedented heterometallic bicyclic architectures with a high level of constitutional control. The methodology relies on the coordination directionality, and the stoichiometry of the individual precursor units, as well as on the difference of the coordination preference of the associated metal ions. As a proof-of-concept example, two aesthetically pleasing Fe–Pt heterometallic bicyclic metallacycles **6a** and **6b**, consisting of nine communicative components from four unique species, were prepared in ca. 70% isolated yields and fully characterized by multinuclear NMR, 2D NMR, electrospray ionization time-of-flight mass, and UV–vis spectroscopies. Furthermore, density functional theory based computations suggest that each of these supramolecular constructs encompasses two twisted [organo–Pt(II)←pyridine] coordination based irregular hexagons that are joined via a robust [terpyridine→Fe(II)←terpyridine] hinge.

Coordination-driven supramolecular synthesis in the past 3 decades was a two-component methodology, wherein rigid electron-poor metal acceptors combine with rigid electron-rich organic donors based on the complementary bonding directionalities that lead to the formation of numerous well-defined supramolecular coordination complexes (SCCs), including two-dimensional (2D) metallacycles and three-dimensional (3D) metallacages.^{1–3} These supramolecular structures due to their adaptable cavities have produced a large number of functional systems, capable of acting as catalysts,⁴ optical materials,⁵ chemical sensors,⁶ drug transporters,⁷ theranostic agents,⁸ and so on. Nevertheless, the structural diversity as well as the functionality that can be obtained by this approach are limited in scope, because essentially all of these structures are constructed via the repetitive use of a single metal←ligand binding motif. This necessitates the development of new strategies allowing the use of multiple donors and acceptors in a single process, while maintaining the synthetic efficiency similar to that of the two-component self-assembly. However, the use of more than two precursors in a self-assembly reaction engenders additional equilibria, via the possible metal and/or ligand exchange reactions that can eventually generate multiple similar structures.⁹ To furnish a single, discrete architecture rather than a statistical mixture of products, all components need to be encoded with the proper electronic and/or structural

information so that in the desired structure their dynamic linkages remain orthogonal, i.e., noncommunicative.¹⁰ With this in mind, some methodologies have recently been developed by the careful control of steric and/or electronic effects, precursors' stoichiometry, metal-ion coordination specifics, etc., that allow the high-yielding synthesis of species having three or more components in their frameworks.¹¹ For example, we recently employed the higher stability of a [*cis*-protected Pt(II)←pyridine (Py), carboxylate] coordination motif over the corresponding [*cis*-protected Pt(II)←Py, Py] and [*cis*-protected Pt(II)←carboxylate, carboxylate] linkages, in the construction of three component heteroleptic systems: trigonal-, tetragonal-, and hexagonal-prisms.¹² Moreover, the [organo–Pt(II)←Py] and [organo–Pt(II)←carboxylate] based coordination motifs can be merged with other noncovalent interactions, such as hydrogen bonding and electrostatic interactions, leading to the formation of sophisticated mechanically interlocked molecules (MIMs) or supramolecular polymers (SPs).¹³

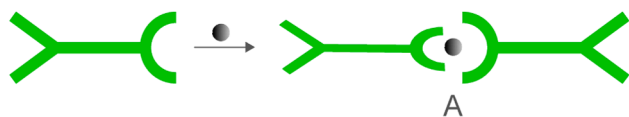
The syntheses of bicyclic architectures are scarce in supramolecular chemistry, although their covalent analogues are omnipresent in natural products and in drug molecules.¹⁴ The groups of Newkome¹⁵ and Stang¹⁶ have recently prepared some fused metallacycles using a vertex-overlapping strategy, wherein one multitopic donor was employed as the common vertices of two polygons. To the best of our knowledge, this has been the only supramolecular approach to obtain bicyclic architectures. In an effort to extend the latter family, we herein demonstrate a novel methodology that results in the self-assembly of twisted heterometallic bicyclic architectures, as shown in Scheme 1. Specifically, this two-step approach combines the concept of “complex-as-a-ligand” strategy¹⁷ and the “stoichiometric controlled multicomponent self-assembly”¹⁶ in a single process, in which the formation of a robust, yet dynamic, metalloligand (A in Scheme 1) is the first step. This metalloligand acts as the hinge and contains additional ligands suitable for preparing the desired rings/cages, in the next step, when mixed with a complementary second metal species and a ligand, at the correct stoichiometric ratio. The orthogonality of these metal←ligand interactions as well as the use of the correct stoichiometry and directionality of the individual precursor units are necessary. Notably, these bicyclic SCCs are not only unique from an aesthetic point of view but also have the prospect of displaying distinct photophysical, electrochemical, and magnetic properties as heterometallic constructs.¹⁸

Received: November 16, 2016

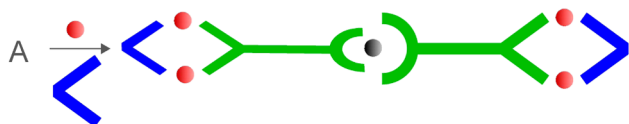
Published: February 2, 2017

Scheme 1. Two-Step Approach for Preparing Unique Heterometallic Bicyclic Architectures

Step I



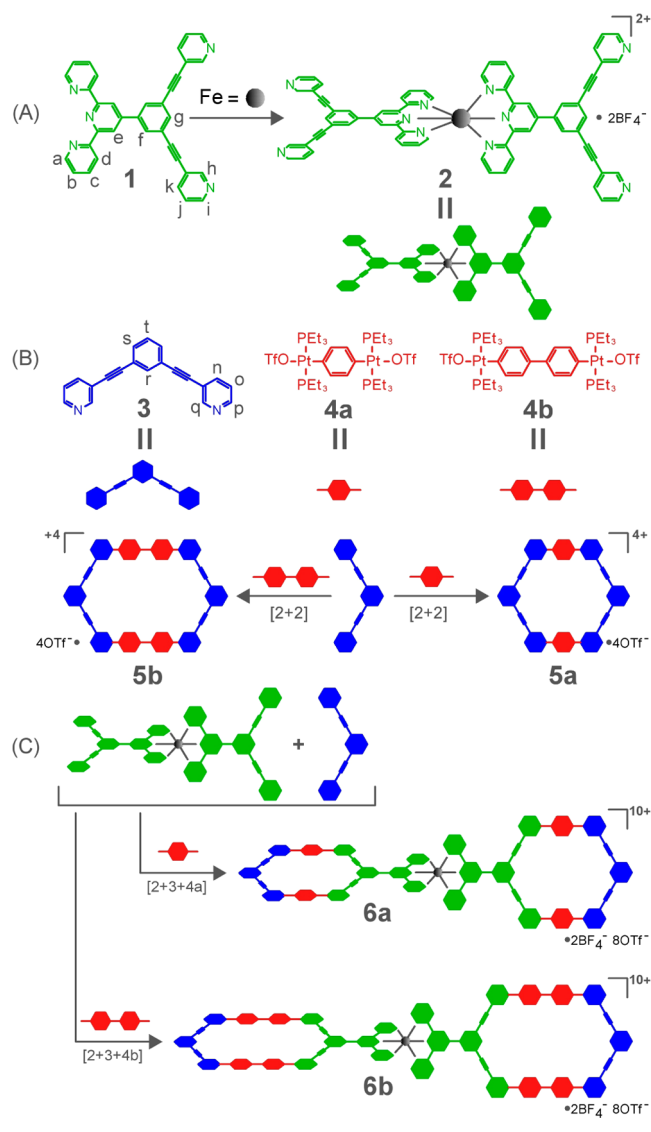
Step II



As a proof-of-concept, the synthesis of two Fe–Pt heterometallic bicyclic metallacycles **6a** and **6b**, bearing two [organo–Pt(II)←Py] coordination based irregular hexagons that are joined by a [terpyridine→Fe(II)←terpyridine] hinge, are described herein. The selection of precursors was influenced by a number of facts: (i) Fe(II) ions generally prefer an octahedral arrangement of six donor atoms,^{19a} whereas the valence of a bis(phosphine)organo–Pt(II) acceptor can be satisfied by a pyridine ligand.^{19b} These properties should support the metal–ligand combinations of **6a** and **6b**, because the other possible alternatives would violate the maximum site occupancy rule²⁰ and are also disfavored on entropic grounds; (ii) the overall association constants (*K*) of [terpyridine→Fe(II)←terpyridine] based motifs are in the range of ca. 10^{16} – 10^{17} , making **2** suitable as the hinge;²¹ (iii) based on the tenets of the “directional bonding approach”^{1a} the coordination directionality of the hinge **2** and ligand **3** are compatible to that of the acceptor **4a** or **4b**. This should facilitate the formation of the required [2+2] hexagons; (iv) both [organo–Pt(II)←Py] and [terpyridine→Fe(II)←terpyridine] binding motifs are kinetically labile, thereby allowing the system to undergo self-repair processes to achieve the thermodynamically controlled superstructure.

To optimize the synthetic conditions for **6a** and **6b**, we first prepared and characterized the metalloligand **2**, and two model irregular hexagons **5a** and **5b** that closely mimic the coordination motifs of the targeted bicyclic metallacycles (Scheme 2). The terpyridine–pyridine hybrid ligand **1** was synthesized via a Pd-catalyzed Sonogashira coupling reaction between 4′-(3,5-dibromophenyl)-2,2′:6′,2″-terpyridine and 3-ethynylpyridine (Scheme S1, see SI); whereas the other precursors **3**, **4a**, and **4b** were prepared by adopting literature procedures.²² Stirring a mixture of ligand **1** and Fe(BF₄)₂·6H₂O in a 2:1 molar ratio in CH₂Cl₂/CH₃CN (*v:v* = 1:1) at room temperature for 1 h, led to the formation of metalloligand **2**, in quantitative yield. Likewise, the model metallacycles **5a** and **5b** were constructed in nearly quantitative yields by combining the “clip” (0°) donor **3** and 180° organo–Pt(II) acceptor **4a** or **4b** in a 1:1 molar ratio in DMSO.

The formation of these SCCs was established by a suite of spectroscopic techniques, including multinuclear NMR (¹H–NMR, ¹⁹FNMR and ³¹P{¹H}–NMR), 2D NMR (¹H–¹H COSY NMR and DOSY NMR), electrospray ionization time-of-flight mass (ESI–TOF–MS), and UV–vis spectroscopies. For example, the ¹H–NMR spectrum of **2** in DMSO-*d*₆ exhibited downfield shifts for the protons H_c ($\Delta\delta$ = 1.05 ppm) and H_d ($\Delta\delta$ = 0.44 ppm) as well as upfield shifts for the protons H_a

Scheme 2. Synthesis of Metalloligand **2** (A), Model Irregular Hexagons **5a** and **5b** (B), and Bicyclic Metallacycles **6a** and **6b** (C)

($\Delta\delta$ = 1.47 ppm) and H_b ($\Delta\delta$ = 0.27 ppm) as compared to those observed in the free ligand **1** in the same solvent, consistent with the formation of its [terpyridine→Fe(II)←terpyridine] motif.²³ At the same time, the protons H_h–H_k of the pyridine cores of **2** have experienced no significant shifts from the free ligand **1**, indicating that they are not engaged in metal-complexation. Similarly, in the ¹H–NMR spectra of **5a** and **5b**, signals corresponding to the central ring (H_r–H_e) of the ligand **3** were located in a similar region to those of the free ligand, while the pyridyl protons (H_o–H_q) underwent downfield shifts, due to the loss of electron density that occurs upon the [organo–Pt(II)←Py] motifs formation. Specifically, the latter set of protons appeared, respectively, at δ = 7.83 ppm, δ = 8.83 ppm and δ = 8.94 ppm in **5a** and at δ = 7.85 ppm, δ = 8.87 ppm and δ = 8.99 ppm in **5b**. The ³¹P{¹H}–NMR spectra of **5a** and **5b** exhibited sharp singlets at δ = 12.5 ppm and δ = 13.9 ppm, respectively, with concomitant ¹⁹⁵Pt satellites, in accordance with their single phosphorus environments. ESI–TOF–MS spectrometry provided evidence about the stoichiometry of these SCCs. In the ESI–TOF–MS spectra of **2** = [Fe(1)₂–

$(\text{BF}_4)_2$, **5a** = $[(\mathbf{4a})_2(\mathbf{3})_2](\text{OTf})_4$ and **5b** = $[(\mathbf{4b})_2(\mathbf{3})_2](\text{OTf})_4$, peaks at m/z = 539.14, 1367.90 and 1444.42 Da, corresponding to $[\mathbf{2} - 2\text{BF}_4]^{2+}$, $[\mathbf{5a} - 2\text{OTf}]^{2+}$ and $[\mathbf{5b} - 2\text{OTf}]^{2+}$, respectively, supporting the corresponding structures as described in Scheme 2.

Next, we examined the synthesis of bicyclic architectures **6a** and **6b**, by following a procedure outlined in Scheme 2C. Accordingly, the preassembled metalloligand **2**, 180° diplatinum acceptor **4a** or **4b** and ligand **3** were dissolved in DMSO in a 1:4:2 molar ratio and heated at 70 °C for 24 h. The products were thereafter isolated in ca. 70% yields as purple solids, using a technique that includes first precipitation and then centrifugation (see SI for details). The ESI-TOF-MS (Figures 1A, S23, and S33) analysis established that the

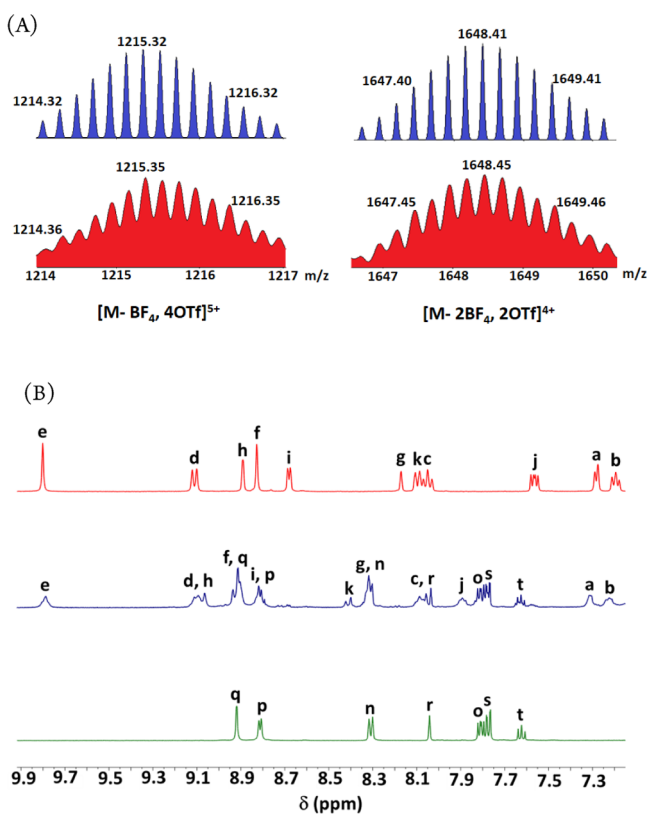


Figure 1. (A) Experimental (red) and calculated (blue) ESI-TOF-MS spectra of bicyclic metallacycles **6a** (left) and **6b** (right). (B) Comparison of the partial ^1H NMR spectra (room temperature, 400 MHz, DMSO- d_6) of (top) **2**; (middle) **6a**; (bottom) **5a**.

stoichiometry of these isolated materials are as **6a** = $[\text{Fe}(\mathbf{1})_2(\mathbf{4a})_4(\mathbf{3})_2](\text{OTf})_8(\text{BF}_4)_2$ and **6b** = $[\text{Fe}(\mathbf{1})_2(\mathbf{4b})_4(\mathbf{3})_2](\text{OTf})_8(\text{BF}_4)_2$, respectively. Specifically, in the ESI-MS spectrum for **6a**, four isotopically well resolved peaks at m/z = 1215.55 Da for $[\mathbf{6a} - \text{BF}_4, 4\text{OTf}]^{5+}$, 1541.42 Da for $[\mathbf{6a} - 4\text{OTf}]^{4+}$, 1556.67 Da for $[\mathbf{6a} - \text{BF}_4, 3\text{OTf}]^{4+}$ and 1572.14 Da for $[\mathbf{6a} - 2\text{BF}_4, 2\text{OTf}]^{4+}$, were observed that are consistent with the stoichiometry. Whereas the composition of **6b** was confirmed by the peaks at m/z = 1288.33 Da for $[\mathbf{6b} - 2\text{BF}_4, 3\text{OTf}]^{5+}$, 1616.93 Da for $[\mathbf{6b} - 4\text{OTf}]^{4+}$, 1632.42 Da for $[\mathbf{6b} - \text{BF}_4, 3\text{OTf}]^{4+}$ and 1647.66 Da for $[\mathbf{6b} - 2\text{BF}_4, 2\text{OTf}]^{4+}$. The multinuclear NMR and 2D NMR data also agreed with these structural assignments. For instance, the previously uncomplexed H_h – H_k protons (vide supra) of **2** underwent significant downfield shifts in **6a/6b** and appeared in a similar region to

those of the H_o – H_q protons of the hexagon **5a/5b** (Scheme 2). This suggests that the H_h – H_j protons of **6a/6b** are involved in a [organo–Pt(II)←Py] type complexation. To confirm further the presence of the other two putative metal–ligand combinations of **6a** and **6b** (Scheme 2C), we compared their ^1H NMR spectra with that of the metalloligand **2**, as well as with that of the corresponding model hexagon **5a** or **5b** (Figures 1B, S5, S8, and S14). Both data suggested that the coordination motifs of **2** and **5a/5b** are preserved in these bicyclic architectures; nevertheless, the diagnostic protons H_a – H_e and H_o – H_q experienced some minute shifts (ca. $\Delta\delta$ = 0.1 ppm) in **6a** and **6b**. Considering the structures of **6a** and **6b**, we expect to see two closely separated singlets in their $^{31}\text{P}\{^1\text{H}\}$ NMR spectra with chemical shifts being similar to those of their corresponding model hexagon **5a** or **5b**, i.e., δ = 12–14 ppm. However, only broad singlets at δ = 13.45 ppm for **6a** and at δ = 14.14 ppm for **6b** with concomitant ^{195}Pt satellites were observed, when the spectra were taken on a 121 MHz machine using DMSO- d_6 solvent at 298 K. Moreover, neither higher field strength (162 MHz) nor VT NMR (0°–45 °C) provided a better resolution of these overlapping peaks, indicating that the chemical environments around the phosphorus atoms are, as expected, very similar in these complexes. The UV–vis spectra of **6a** and **6b** are diagnostic and provide further evidence about their [terpyridine→Fe(II)←terpyridine] binding motifs by showing the characteristic metal–ligand charge transfer (MLCT) bands at ca. 577 nm.²¹ These bands, however, are slightly red-shifted ($\Delta\lambda$ = 1 nm) compared to that of the metalloligand **2**. These data collectively establish that the frameworks of **6a** and **6b** contain nine molecular components from four different species that are held by three different metal←ligand interactions. Most interestingly, the mixing of **1**, Fe^{2+} , **3**, and **4**, at a ratio of 2:1:2:4 respectively, in one pot likewise formed **6** with little or no **5** being observed. At the present time, we do not have an explanation for this remarkable selection and constitutional control. Furthermore, based upon the X-ray evidence²⁴ of precursor **2** the bicyclic products **6** are likely to be twisted.

DOSY NMR spectroscopy was also used to examine the purity of **6a** and **6b**, which showed single vertical traces as expected for pure assemblies. Because the geometrical lengths of the bicyclic architectures are approximately twice that of those of the model hexagons, it is expected that the former should have lower diffusion coefficients than the latter. Indeed, a 2-fold decrease was observed when we compared the diffusion constants ($10^{-10} \text{ m}^2 \text{ s}^{-1}$) for the metallacycles **5a/5b** (1.13/0.86) with that of **6a/6b** (0.56/0.42).

All attempts to obtain single crystals of **6a** and **6b** were unsuccessful. Thus, DFT computations (gas phase; B3LYP; 6-31G** for C, H, N, P; LANL2DZ for Fe, Pt) were performed to gain further insight into their structural characteristics. These results support the proposed bicyclic architectures of **6a** and **6b**, and are in good agreement with their DOSY-derived hydrodynamic radii (see SI). Notably, in both cases the two irregular hexagonal rings are arranged in a perpendicular (ca. 100°) fashion, with separations of ca. 1.0 nm. The length of these bicyclic architectures were determined by the distance between two farthest carbon centers, which appeared as 5.96 nm for **6a** and 6.82 nm for **6b**. Whereas the model hexagons are only 2.29 nm (**5a**) and 2.72 nm (**5b**) in length (see Figures S39–S42).

In conclusion, we have described a general strategy to obtain twisted heterometallic bicyclic architectures by merging the complex-as-a-ligand strategy and the stoichiometry controlled

multicomponent self-assembly in a single process. The validity of this new concept was shown via the synthesis of two Fe–Pt heterometallic bicyclic architectures **6a** and **6b** consisting of four different species. These SCCs were isolated in high yields as well as characterized by a suite of spectroscopic techniques. Hence, the synthesis of unique heterometallic twisted bicyclic architectures has been accomplished for the first time.

■ ASSOCIATED CONTENT

■ Supporting Information

The Supporting Information is available free of charge on the ACS Publications website at DOI: 10.1021/jacs.6b11860.

Experimental details and additional data (PDF)

■ AUTHOR INFORMATION

Corresponding Authors

*h.sehehrpour@utah.edu

*manik.saha@utah.edu

*stang@chem.utah.edu

Notes

The authors declare no competing financial interest.

■ ACKNOWLEDGMENTS

P.J.S. thanks the NSF (Grant 1212799) for financial support. Computational resources are gratefully acknowledged from the Center for High Performance Computing (CHPC) at the University of Utah.

■ REFERENCES

- (1) (a) Cook, T. R.; Stang, P. J. *Chem. Rev.* **2015**, *115*, 7001–7045. (b) Brown, C. J.; Toste, F. D.; Bergman, R. G.; Raymond, K. N. *Chem. Rev.* **2015**, *115*, 3012–3035. (c) McConnell, A. J.; Wood, C. S.; Neelakandan, P. P.; Nitschke, J. R. *Chem. Rev.* **2015**, *115*, 7729–7793. (d) Newkome, G. R.; Moorefield, C. N. *Chem. Soc. Rev.* **2015**, *44*, 3954–3967. (e) Lifschitz, A. M.; Rosen, M. S.; McGuirk, C. M.; Mirkin, C. A. *J. Am. Chem. Soc.* **2015**, *137*, 7252–7261.
- (2) (a) Han, M.; Engelhard, D. M.; Clever, G. H. *Chem. Soc. Rev.* **2014**, *43*, 1848–1860. (b) Saha, M. L.; Neogi, S.; Schmittel, M. *Dalton Trans.* **2014**, *43*, 3815–3834. (c) Mukherjee, S.; Mukherjee, P. S. *Chem. Commun.* **2014**, *50*, 2239–2248. (d) Yoshizawa, M.; Klosterman, J. K. *Chem. Soc. Rev.* **2014**, *43*, 1885–1898. (e) Harris, K.; Fujita, D.; Fujita, M. *Chem. Commun.* **2013**, *49*, 6703–6712. (f) Smulders, M. M. J.; Riddell, I. A.; Browne, C.; Nitschke, J. R. *Chem. Soc. Rev.* **2013**, *42*, 1728–1754.
- (3) (a) Chakrabarty, R.; Mukherjee, P. S.; Stang, P. J. *Chem. Rev.* **2011**, *111*, 6810–6918. (b) Safont-Sempere, M. M.; Fernández, G.; Würthner, F. *Chem. Rev.* **2011**, *111*, 5784–5814. (c) Saalfrank, R. W.; Maid, H.; Scheurer, A. *Angew. Chem., Int. Ed.* **2008**, *47*, 8794–8824. (d) Oliveri, C. G.; Ulmann, P. A.; Wiester, M. J.; Mirkin, C. A. *Acc. Chem. Res.* **2008**, *41*, 1618–1629.
- (4) (a) Kaphan, D. M.; Levin, M. D.; Bergman, R. G.; Raymond, K. M.; Toste, F. D. *Science* **2015**, *350*, 1235–1238. (b) Neelakandan, P. P.; Jiménez, A.; Thoburn, J. D.; Nitschke, J. R. *Angew. Chem., Int. Ed.* **2015**, *54*, 14378–14382.
- (5) (a) Saha, M. L.; Yan, X.; Stang, P. J. *Acc. Chem. Res.* **2016**, *49*, 2527–2539. (b) Neelakandan, P. P.; Jiménez, A.; Nitschke, J. R. *Chem. Sci.* **2014**, *5*, 908–915. (c) Zhang, Q.-W.; Li, D.; Li, X.; White, P. B.; Mecinović, J.; Ma, X.; Agren, H.; Nolte, R. J. M.; Tian, H. *J. Am. Chem. Soc.* **2016**, *138*, 13541–13550.
- (6) (a) Yan, X.; Cook, T. R.; Wang, P.; Huang, F.; Stang, P. J. *Nat. Chem.* **2015**, *7*, 342–348. (b) Chen, L.-J.; Ren, Y.-Y.; Wu, N.-W.; Sun, B.; Ma, J.-Q.; Zhang, L.; Tan, H.; Liu, M.; Li, X.; Yang, H.-B. *J. Am. Chem. Soc.* **2015**, *137*, 11725–11735. (c) Chowdhury, A.; Howlader, P.; Mukherjee, P. S. *Chem. - Eur. J.* **2016**, *22*, 7468–7478. (d) Wang, J.; He, C.; Wu, P.; Wang, J.; Duan, C. *J. Am. Chem. Soc.* **2011**, *133*, 12402–12405.
- (7) (a) Therrien, B.; Süß-Fink, G.; Govindaswamy, P.; Renfrew, A. K.; Dyson, P. J. *Angew. Chem., Int. Ed.* **2008**, *47*, 3773–3776. (b) Lewis, J. E. M.; Gavey, E. L.; Cameron, S. A.; Crowley, J. D. *Chem. Sci.* **2012**, *3*, 778–784. (c) Samanta, S. K.; Moncelet, D.; Briken, V.; Isaacs, L. J. *Am. Chem. Soc.* **2016**, *138*, 14488–14496.
- (8) Grishagin, I. V.; Pollock, J. B.; Kushal, S.; Cook, T. R.; Stang, P. J.; Olenyuk, B. Z. *Proc. Natl. Acad. Sci. U. S. A.* **2014**, *111*, 18448–18453.
- (9) Northrop, B. H.; Zheng, Y.-R.; Chi, K.-W.; Stang, P. J. *Acc. Chem. Res.* **2009**, *42*, 1554–1563.
- (10) Wei, P.; Yan, X.; Huang, F. *Chem. Soc. Rev.* **2015**, *44*, 815–832.
- (11) (a) Saha, M. L.; Schmittel, M. *J. Am. Chem. Soc.* **2013**, *135*, 17743–17746. (b) Wang, S.-Y.; Fu, J.-H.; Liang, Y.-P.; He, Y.-J.; Chen, Y.-S.; Chan, Y.-T. *J. Am. Chem. Soc.* **2016**, *138*, 3651–3654. (c) Howlader, P.; Mukherjee, P. S. *Chem. Sci.* **2016**, *7*, 5893–5899. (d) Gianneschi, N. C.; Masar, M. S., III; Mirkin, C. A. *Acc. Chem. Res.* **2005**, *38*, 825–837.
- (12) Ye, Y.; Cook, T. R.; Wang, S.-P.; Wu, J.; Li, S.; Stang, P. J. *J. Am. Chem. Soc.* **2015**, *137*, 11896–11899.
- (13) (a) Zhou, Z.; Yan, X.; Cook, T. R.; Saha, M. L.; Stang, P. J. *J. Am. Chem. Soc.* **2016**, *138*, 806–809. (b) Yan, X.; Li, S.; Cook, T. R.; Ji, X.; Yao, Y.; Pollock, J. B.; Shi, Y.; Yu, G.; Li, J.; Huang, F.; Stang, P. J. *J. Am. Chem. Soc.* **2013**, *135*, 14036–14039. (c) Ye, Y.; Wang, S.-P.; Zhu, B.; Cook, T. R.; Wu, J.; Li, S.; Stang, P. J. *Org. Lett.* **2015**, *17*, 2804–2807.
- (14) Smith, L. K.; Baxendale, I. R. *Org. Biomol. Chem.* **2015**, *13*, 9907–9933.
- (15) (a) Schultz, A.; Li, X.; Barkakaty, B.; Moorefield, C. N.; Wesdemiotis, C.; Newkome, G. R. *J. Am. Chem. Soc.* **2012**, *134*, 7672–7675. (b) Lu, X.; Li, X.; Wang, J.-L.; Moorefield, C. N.; Wesdemiotis, C.; Newkome, G. R. *Chem. Commun.* **2012**, *48*, 9873–9875.
- (16) (a) Lee, J.; Ghosh, K.; Stang, P. J. *J. Am. Chem. Soc.* **2009**, *131*, 12028–12029. (b) Zhou, Z.; Yan, X.; Saha, M. L.; Zhang, M.; Wang, M.; Li, X.; Stang, P. J. *J. Am. Chem. Soc.* **2016**, *138*, 13131–13134.
- (17) (a) Ryu, J. Y.; Park, Y. J.; Park, H.-R.; Saha, M. L.; Stang, P. J.; Lee, J. *J. Am. Chem. Soc.* **2015**, *137*, 13018–13023. (b) Brusilowski, B.; Dzyuba, E. V.; Troff, R. W.; Schalley, C. A. *Chem. Commun.* **2011**, *47*, 1830–1832.
- (18) (a) Liu, G.; Zeller, M.; Su, K.; Pang, J.; Ju, Z.; Yuan, D.; Hong, M. *Chem.—Eur. J.* **2016**, *22*, 17345–17350. (b) Metherell, A. J.; Ward, M. D. *Chem. Commun.* **2014**, *50*, 10979–10982. (c) Reichel, F.; Clegg, J. K.; Gloe, K.; Gloe, K.; Weigand, J. J.; Reynolds, J. K.; Li, C.-G.; Aldrich-Wright, J. R.; Kepert, C. J.; Lindoy, L. F.; Yao, H.-C.; Li, F. *Inorg. Chem.* **2014**, *53*, 688–690.
- (19) (a) Schultz, A.; Li, X.; McCusker, C. E.; Moorefield, C. N.; Castellano, F. N.; Wesdemiotis, C.; Newkome, G. R. *Chem. - Eur. J.* **2012**, *18*, 11569–11572. (b) Seidel, S. R.; Stang, P. J. *Acc. Chem. Res.* **2002**, *35*, 972–983.
- (20) Kramer, R.; Lehn, J.-M.; Marquis-Rigault, A. *Proc. Natl. Acad. Sci. U. S. A.* **1993**, *90*, 5394–5398.
- (21) Dobrawa, R.; Ballester, P.; Saha-Möller, C. R.; Würthner, F. *ACS Symposium Series.* **2006**, *928*, 43–62.
- (22) Li, Z.-Y.; Zhang, Y.; Zhang, C.-W.; Chen, L.-J.; Wang, C.; Tan, H.; Yu, Y.; Li, X.; Yang, H.-B. *J. Am. Chem. Soc.* **2014**, *136*, 8577–8589.
- (23) The downfield shifts presumably occurred due to a loss of the electron density from the terpyridine cores upon metal coordination, whereas the octahedral arrangement of the six donor atoms at the Fe(II) center in **2** places the H_a and H_b protons of one terpyridine ring in the shielding zone of the other ring. Thus, these protons underwent upfield shifts.
- (24) Yang, J.; Clegg, J. K.; Jiang, Q.; Lui, X.; Yan, H.; Zhong, W.; Beves, J. E. *Dalton Trans.* **2013**, *42*, 15625–15636.